

Compound droplet in extensional and paraboloidal flows

D. Palaniappan

Institut für Theoretische Physik, RWTH Aachen, Templergraben 55, 52062 Aachen, Germany

Prabir Daripa^{a)}

Department of Mathematics, Texas A&M University, College Station, Texas 77843-3368

(Received 2 July 1999; accepted 30 June 2000)

Exact analytical solutions are found for the steady state creeping flow in and around a vapor–liquid compound droplet, consisting of two orthogonally intersecting spheres of arbitrary radii (a and b), submerged in axisymmetric extensional and paraboloidal flows of fluid with viscosity $\mu^{(1)}$. The solutions are presented in singularity form with the images located at three points: the two centers of the spheres and their common inverse point. The important results of physical interest such as drag force and stresslet coefficient are derived and discussed. These flow properties are characterized by two parameters, namely the dimensionless viscosity parameter: $\Lambda = \mu^{(2)}/(\mu^{(1)} + \mu^{(2)})$, and the dimensionless parameter: $\beta = b/a$, where $\mu^{(2)}$ is the viscosity of the liquid in the sphere (part of the compound droplet) with radius b . We find that for some extensional flows, there exists a critical value of $\beta = \beta_c$ for each choice of Λ in the interval $0 \leq \Lambda \leq 1$ such that the drag force is negative, zero or positive depending on whether $\beta < \beta_c$, $\beta = \beta_c$, or $\beta > \beta_c$ respectively. For other extensional flows, the drag force is always positive. The realization of these various extensional flows by simply changing the choice of the origin in our description of the undisturbed flow field is also discussed. In extensional flows where the drag force is always positive, we notice that this drag force D_e for vapor–liquid compound droplet is maximum when $\beta \approx 1$ (i.e., two spheres have almost the same radii). Moreover, we find the drag force D_e is a monotonic function of Λ , i.e., the drag force for vapor–liquid compound droplet lies between vapor–vapor and vapor-rigid assembly limits. We also find that the maximum value of the drag in paraboloidal flow depends on the viscosity ratio Λ and significantly on the liquid volume in the dispersed phase. © 2000 American Institute of Physics. [S1070-6631(00)01310-6]

I. INTRODUCTION

The study of hybrid multiphase droplets is of great interest in many areas of science and technology. These droplets occur in processes such as melting of ice particles in the atmosphere, liquid membrane technology as well as in other industrial operations. Furthermore, the compound droplets are also found to exist in lipid bilayer¹ and polymer grafted² membranes in concentrated solutions. The fluid mechanics of such droplets is discussed for instance in Avedisian *et al.*,³ Johnson and Sadhal,⁴ and Sadhal *et al.*⁵ among many others. In electrostatics, the compound (merging) objects are modeled as two overlapping spherical surfaces and their responses to applied electric fields are explored. In this case, the solutions of Laplace equation provide excellent theoretical results as explained in Jones⁶ and Radchik *et al.*⁷ However, the fluid mechanics of such objects (in the limit of zero Reynolds number) depends on the solutions of vector biharmonic equations.

Solutions of Stokes-flow problems, in which inertial effects are negligible in comparison with the viscous effects have been studied since the time of Stokes⁸ who himself solved the problem of a translating sphere. Many years later Lamb⁹ presented the general solution of Stokes equations by

the use of spherical harmonics. The motion of ellipsoidal particles in a viscous fluid has also been treated using sophisticated analysis of ellipsoidal harmonics. For references on these works together with some perspectives on analytical and numerical techniques for Stokes-flow past submerged bodies, the reader is directed to the standard monographs on the subject.^{10–12} The singularity method, which was originated by Lorentz,¹³ has also been applied by many to consider the fluid motion about nonspherical particles and Chwang and Wu¹⁴ has exploited it further and gave references to previous works. Payne and Pell¹⁵ treated the creeping flow problems of axially symmetric bodies by employing a stream function technique. Comparing the singularity method with the other methods, one finds that the former is simpler and more elegant. Surprisingly, only ellipsoids and spheroids have received more attention in earlier studies with the singularity method. For bodies consisting of overlapping surfaces, the solution in singularity form was found only recently by Palaniappan and Kim.¹⁶ There is another notable work by Vuong and Sadhal¹⁷ concerning the translation and growth of a compound drop. The cited authors used the toroidal coordinates and solved the problem analytically for arbitrary contact angle. The solutions and the drag are expressed in terms of infinite integrals that needed further numerical computations. However, in those studies,^{16,17} only the problem of uniform flow past a partially encapsulated

^{a)}Author for correspondence.

droplet was discussed to illustrate the basic idea.

Interests in droplet motions in non-uniform velocity fields stem from a variety of industrial and naturally occurring processes involving suspended particles. For instance, the motion of cells in capillaries and processing emulsions is of considerable interest in many areas. Furthermore, the problem of cross-stream migration of suspended particles due to hydrodynamic interactions has also attracted attention.¹⁸⁻²⁰ But the attention is focussed only for spheres in these studies. In the case of bodies attached to surfaces, the analytical approach has been avoided owing to the difficulty to describe those geometries mathematically. As a result, numerical solutions are sought for problems involving drops attached to surfaces.²¹

Motivated by the above, in the present analysis we calculate the detailed Stokes-flow past a compound droplet immersed in axisymmetric extensional and paraboloidal flow fields. Analytic solutions for the two-sphere assembly are obtained in closed forms in terms of the stream function in spherical coordinates. The required singularities for the solutions are obtained by repeated application of the sphere theorems developed previously.²² The final solutions are presented in singularity forms with the image singularities located at the two centers of the spheres and their common inverse point inside the two-sphere assembly. The drag and the stresslet coefficients follow directly from the solutions without integrating the surface stresses.

The organization of the paper is as follows. We start with the geometrical description of the compound droplet together with the statement of the problem and the boundary conditions. In Sec. III, we reformulate the problem and also derive the boundary conditions in terms of stream function. Then using the sphere theorems, we construct the solution in singularity form for the two non-uniform flow fields in subsections III A and III B. It is clear from the present method that the toroidal coordinate system is not required to find the solutions for this special geometry. The discussion of the results including derivation of drag and stresslet coefficient are presented in Sec. IV. The additional characteristics of the drag in extensional flow are provided in Sec. V followed by the concluding remarks in Sec. VI.

II. PROBLEM STATEMENT

The schematic of the compound droplet is depicted in Fig. 1. The two-sphere assembly, denoted by Γ , consists of two unequal spheres S_a and S_b of radii a and b intersecting orthogonally with centers O and O' , respectively. The two centers share a common inverse point D such that $OD = a^2/c$, $DO' = b^2/c$, $c^2 = a^2 + b^2$ where $OO' = c$. The geometry drawn in Fig. 1 is more realistic if one of the spheres is a solid which is a special case of our analysis. It should be remarked that the interface AB adjoining the two segments will have curvature different from that of the sphere S_a for a fluid-fluid system. We use the spherical polar coordinates (r, θ, ϕ) , (r', θ', ϕ) , and (R, Θ, ϕ) of any point outside the assembly Γ with O , O' and D as origins, respectively. The geometrical relations connecting the coordinates are

$$r^2 = r'^2 + 2cr' \cos \theta' + c^2, \tag{1}$$

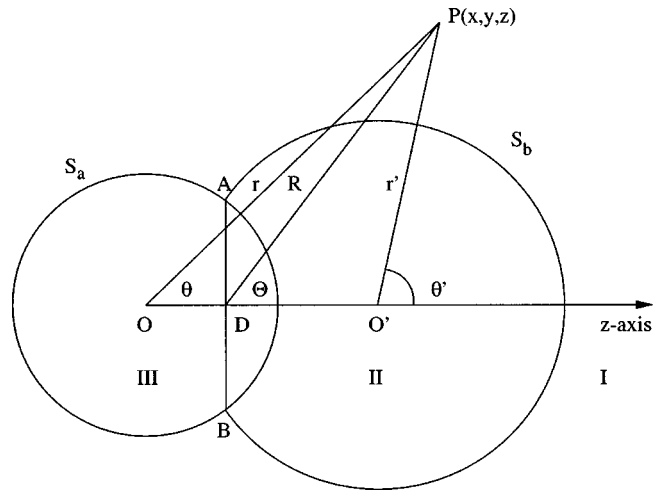


FIG. 1. The two-sphere assembly Γ .

$$r'^2 = r^2 - 2cr \cos \theta + c^2, \tag{2}$$

$$R^2 = r^2 - 2 \frac{a^2}{c} r \cos \theta + \frac{a^4}{c^2}, \tag{3}$$

$$= r'^2 + 2 \frac{b^2}{c} r' \cos \theta' + \frac{b^4}{c^2}.$$

On the spheres S_a and S_b , r' and r reduce to

$$r' = \frac{c}{a} R \quad \text{on } r = a, \tag{4}$$

$$r = \frac{c}{b} R \quad \text{on } r' = b. \tag{5}$$

The sphere S_b contains a liquid (with viscosity different from the outside fluid region) and sphere S_a is a bubble containing vapor. We designate the fluid region exterior to Γ as I and the spherical regions S_b and S_a and II and III , respectively. The surface tension forces are assumed to be large enough to keep the interfaces in a spherical shape. As mentioned in Palaniappan and Kim,¹⁶ the vapor-liquid configuration exists at rest with contact angle approximately 90° if $\gamma_{I,II} \approx \gamma_{II,III} \gg \gamma_{I,III}$ which is in agreement with Laplace law on all interfaces. Here the γ 's denote the surface tension at the interface separating regions.

The Reynolds number of the flow fields is assumed to be small so that all inertial effects are neglected. The governing equations for fluid flow are the Stokes equations or creeping flow equations,

$$\mu^{(i)} \nabla^2 \mathbf{q}^{(i)} = \nabla p^{(i)}, \quad \nabla \cdot \mathbf{q}^{(i)} = 0, \quad (i = 1, 2), \tag{6}$$

where $i = 1, 2$ is used to denote the dispersed and the continuous-phase liquids, respectively, $\mathbf{q}^{(i)}$, $p^{(i)}$, and $\mu^{(i)}$ are the velocities, pressures, and viscosities in the respective phases. The boundary and interface conditions are summarized below:

- far from the droplet, velocity, and pressure are that of the basic flow;
- zero normal velocity on $r = a$ and $r' = b$;

- continuity of tangential velocity and shear stress at liquid–liquid interface I–II at $r' = b$;
- zero shear-stress at $r = a$.

The governing Stokes equations (6) subject to the asymptotic and boundary as well as interface conditions stated above constitute a well-posed problem whose solution provides the velocity and pressure prevailing in the presence of the compound droplet.

III. EXACT SOLUTIONS

We consider two separate problems namely, compound droplet suspended in axisymmetric (i) extensional and (ii) paraboloidal flows. As the flow is axisymmetric about z -axis, we use Stokes stream function formulation which requires the solution of the fourth-order scalar equation

$$L_{-1}^2 \psi = 0, \tag{7}$$

where L_{-1} is the axisymmetric Stokes operator defined by

$$\begin{aligned} L_{-1} &= \frac{\partial^2}{\partial r^2} + \frac{1 - \eta^2}{r^2} \frac{\partial^2}{\partial \eta^2}, \\ &= \frac{\partial^2}{\partial r'^2} + \frac{1 - \eta'^2}{r'^2} \frac{\partial^2}{\partial \eta'^2}, \end{aligned} \tag{8}$$

for the coordinates (r, θ) with $\eta = \cos \theta$ and (r', θ') with $\eta' = \cos \theta'$ respectively. Now the velocity components in terms of the stream function are given by

$$q_r^{(i)} = \frac{1}{r^2 \sin \theta} \frac{\partial \psi^{(i)}}{\partial \theta}, \tag{9}$$

$$q_\theta^{(i)} = -\frac{1}{r \sin \theta} \frac{\partial \psi^{(i)}}{\partial r}, \tag{10}$$

and the pressure is obtained from

$$\frac{\partial p^{(i)}}{\partial r} = -\frac{\eta}{r^2 \sin \theta} \frac{\partial}{\partial \theta} (L_{-1} \psi^{(i)}), \tag{11}$$

$$\frac{\partial p^{(i)}}{\partial \theta} = \frac{\eta}{\sin \theta} \frac{\partial}{\partial r} (L_{-1} \psi^{(i)}). \tag{12}$$

The boundary conditions in terms of the stream function become

$$\psi^{(1)} = 0 = \frac{\partial}{\partial r} \frac{1}{r^2} \frac{\partial \psi^{(1)}}{\partial r}, \tag{13}$$

on the part of the droplet where $r = a$ and

$$\psi^{(1)} = 0 = \psi^{(2)}, \tag{14}$$

$$\frac{\partial \psi^{(1)}}{\partial r'} = \frac{\partial \psi^{(2)}}{\partial r'}, \tag{15}$$

$$\mu^{(1)} \left(\frac{\partial}{\partial r'} \frac{1}{r'^2} \frac{\partial \psi^{(1)}}{\partial r'} \right) = \mu^{(2)} \left(\frac{\partial}{\partial r'} \frac{1}{r'^2} \frac{\partial \psi^{(2)}}{\partial r'} \right), \tag{16}$$

on the remaining part of the droplet where $r' = b$. Below, we obtain the exact solutions for the two problems.

A. Extensional flow past a compound droplet

We consider a stationary compound droplet with boundary Γ , part of which is filled with another liquid of different viscosity immersed in an axisymmetric shear flow. The stream function corresponding to this axisymmetric flow is $\psi_0 = \alpha r^3 \sin^2 \theta \cos \theta$, where α is a shear constant and θ , unless otherwise mentioned below, refers to the polar angle measured counterclockwise at O from the axis of symmetry of the droplet as shown in Fig. 1. It is worth pointing out that if the angle θ is measured with respect to a different origin along the axis, then the ψ_0 as given above will correspond to a different extensional flow. Therefore this stream function ψ_0 can be used to refer to several extensional flows simply shifting the point O for the purposes of measurement of angle θ .

We now determine the perturbed stream function in the presence of the compound droplet. In order to construct the image system for the two-sphere assembly we write the modified external flow as

$$\psi^{(1)} = \psi_0 + \psi_a + \psi_b + \psi_{ab}. \tag{17}$$

The expression for ψ_a consists of the image of ψ_0 in the sphere S_a which is a stress-free. Applying the sphere theorem [see Eq. (21) in Palaniappan *et al.*²²] for a shear-free spherical surface, we find that the image is a stresslet located at the point O (see Fig. 1):

$$\psi_a = -\alpha a^3 \sin^2 \theta \cos \theta. \tag{18}$$

We again apply the sphere theorem²² to find the image of ψ_0 in the sphere S_b . It can be seen that the image system in this case consists of four singularities viz. Stokeslet, stresslet, degenerate Stokes-quadrupole (potential-doublet) and degenerate Stokes-octupole all located at O' (see Fig. 1). The expression for ψ_b may be written as

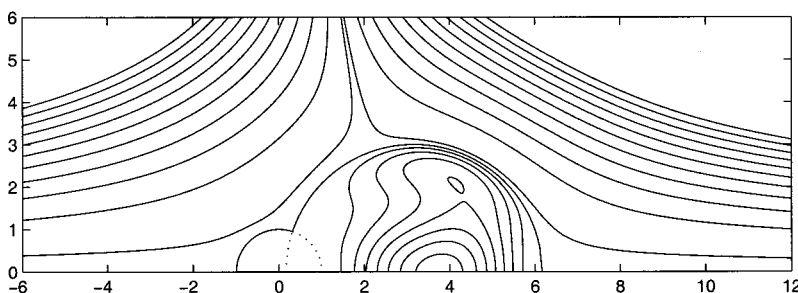


FIG. 2. Typical streamline pattern for flow around a vapor–liquid compound droplet in extensional flow.

$$\begin{aligned} \psi_b = \Lambda \left[\left(-\frac{5b^3}{2} \cos \theta' + \frac{3b^5}{2} \frac{\cos \theta'}{r'^2} - \frac{3bc}{2} r' \right. \right. \\ \left. \left. + \frac{b^3c}{2r'} \right) \alpha \sin^2 \theta' \right] - (1 - \Lambda) [\alpha b^3 \sin^2 \theta' \cos \theta' \\ + abc r' \sin^2 \theta'], \end{aligned} \tag{19}$$

where $\Lambda = \mu^{(2)}/(\mu^{(1)} + \mu^{(2)})$. The next step is to find the image of ψ_a and ψ_b in S_b and S_a respectively. Once again applying the sphere theorem, the images for a stresslet in S_b are found to be Stokeslet, Stokes-doublet, Stokes-quadrupole, degenerate Stokes-quadrupole and degenerate Stokes-octupole all located at D (see Fig. 1). The strengths of

these singularities depend on radii, the distance between the centers and the viscosity ratio. The resulting expression is written as

$$\begin{aligned} \psi_{ab} = \Lambda \left[\frac{3a^5b}{c^4} R - \frac{a^3b^3}{2c^3} \left(9 \frac{a^2}{c^2} - 2 \right) \cos \Theta - \frac{a^5b^3}{2c^4R} \left(3 \frac{a^2}{c^2} - 2 \right) \right. \\ \left. + \frac{3a^5b^5}{c^6} \frac{\cos^2 \Theta}{R} + \frac{3a^7b^5}{2c^7} \frac{\cos \Theta}{R^2} \right] \alpha \sin^2 \Theta + (1 - \Lambda) \\ \times \left[\frac{a^3b}{c^2} R - \frac{a^3b^3}{c^3} \cos \Theta \right] \alpha \sin^2 \Theta. \end{aligned} \tag{20}$$

The images of ψ_b in S_a (obtained using the same procedure as before) are found to be the same as in Eq. (20) and so we have $\psi_{ab} = \psi_{ba}$. Therefore the complete stream function for the flow exterior to Γ is

$$\begin{aligned} \psi^{(1)}(r, \theta) = \alpha r^3 \sin^2 \theta \cos \theta - \alpha a^3 \sin^2 \theta \cos \theta + \Lambda \left[\left(-\frac{5b^3}{2} \cos \theta' + \frac{3b^5}{2} \frac{\cos \theta'}{r'^2} - \frac{3bc}{2} r' + \frac{b^3c}{2r'} \right) \alpha \sin^2 \theta' \right] \\ - (1 - \Lambda) [\alpha b^3 \sin^2 \theta' \cos \theta' + abc r' \sin^2 \theta'] + \Lambda \left[\frac{3a^5b}{2c^4} R - \frac{a^3b^3}{2c^3} \left(9 \frac{a^2}{c^2} - 2 \right) \cos \Theta - \frac{a^5b^3}{2c^4R} \left(3 \frac{a^2}{c^2} - 2 \right) \right. \\ \left. + \frac{3a^5b^5}{c^6} \frac{\cos^2 \Theta}{R} + \frac{3a^7b^5}{2c^7} \frac{\cos \Theta}{R^2} \right] \alpha \sin^2 \Theta + (1 - \Lambda) \left[\frac{a^3b}{c^2} R - \frac{a^3b^3}{c^3} \cos \Theta \right] \alpha \sin^2 \Theta, \end{aligned} \tag{21}$$

and the stream function for the internal flow is

$$\psi^{(2)}(r, \theta) = (1 - \Lambda) \frac{(r'^2 - b^2)}{2b^2} \left[-3 + 2r' - \frac{(r'^2 - b^2)}{2} L_{-1} \right] (r^3 - a^3) \alpha \sin^2 \theta \cos \theta, \tag{22}$$

where L_{-1} is defined as in Eq. (8). Thus by repeated application of sphere theorems developed previously in the literature, we have determined the stream functions for the dispersed and continuous phases. It is important to note that the solutions are obtained in singularity form.

Some typical streamline patterns inside and outside the compound droplet are shown in Fig. 2. We discuss other important physical quantities extracted from this solution in Sec. IV.

B. Paraboloidal flow past a compound droplet

We now consider the compound droplet submerged in an axisymmetric paraboloidal flow. The stream function corresponding to the unbounded paraboloidal flow is $\psi_0 = Kr^4 \sin^4 \theta$, where K is a constant. The perturbed stream function may be obtained as explained in the previous subsection. The respective images can be derived using the same method discussed in the previous subsection. The final expressions for the stream functions in both regions are as follows. For the fluid exterior to the droplet, we have

$$\begin{aligned} \psi^{(1)}(r, \theta) = Kr^4 \sin^4 \theta - K \frac{a^5}{r} \sin^4 \theta + \Lambda \left[-\frac{7b}{2r'} \sin^2 \theta' + \frac{5b^3}{2r'^3} \sin^2 \theta' + \frac{4b}{r'} - \frac{2b^3}{r'^3} - \frac{2r'}{b} \right] Kb^4 \sin^2 \theta' - (1 - \Lambda) K \frac{b^5}{r'} \sin^4 \theta' \\ + \Lambda \left[\frac{2a^5b^3}{c^5} R - \frac{8a^5b^5}{c^6} \cos \Theta - \frac{4a^7b^5}{c^7R} + \frac{a^5b^5}{2c^5} \left(7 - 5 \frac{b^2}{c^2} \right) \frac{\sin^2 \Theta}{R} - \frac{5a^7b^7}{c^8} \frac{\sin^2 \Theta \cos \Theta}{R^2} - \frac{5a^9b^7}{2c^9} \frac{\sin^2 \Theta}{R^3} \right. \\ \left. + \frac{8a^5b^7}{c^7} \frac{\cos^2 \Theta}{R} + \frac{8a^7b^7}{c^8} \frac{\cos \Theta}{R^2} + \frac{2a^9b^7}{c^9R^3} \right] K \sin^2 \Theta + (1 - \Lambda) K \frac{a^5b^5}{c^5} \frac{\sin^4 \Theta}{R}, \end{aligned} \tag{23}$$

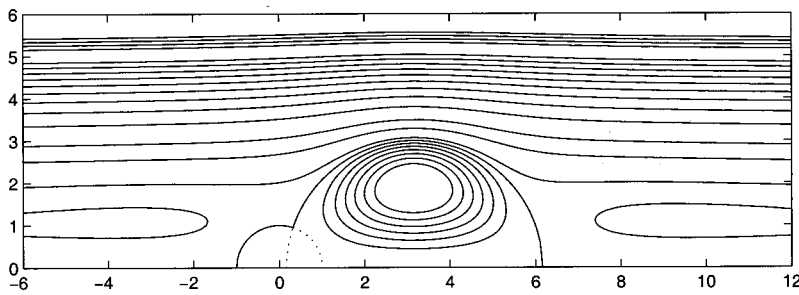


FIG. 3. Typical streamline pattern for flow around a vapor-liquid compound droplet in paraboloidal flow.

and for the fluid inside the droplet, we have

$$\psi^{(2)}(r, \theta) = (1 - \Lambda) \frac{(r'^2 - b^2)}{2b^2} \left[-3 + 2r' - \frac{(r'^2 - b^2)}{2} L_{-1} \right] \times \left(1 - \frac{a^5}{r^5} \right) Kr^4 \sin^4 \theta, \tag{24}$$

where L_{-1} is defined in Eq. (8). The image system for the external flow consists of (i) potential-doublet and Stokes-quadrupole at O ; (ii) Stokeslet, potential-doublet, Stokes and potential quadrupoles and potential octupole at O' ; and (iii) Stokeslet, Stokes and potential doublets, Stokes and potential quadrupoles, and Stokes and potential octupoles at D . The strengths of these singularities depend on the radii a and b , distance between the centers and the viscosity ratio. Some typical streamline patterns inside and outside the compound droplet are shown in Fig. 3. It can be seen that the flow has two ‘backflow’ regions on both sides of the compound droplet which may be due to geometrical effect. We discuss the drag in paraboloidal flow briefly in the next section.

We observe that the solutions for a compound droplet suspended in extensional and paraboloidal flows involve only point image singularities. The locations of these images are the two centers O , O' , and their common inverse point D . For the extremal values of Λ the solutions (21)–(24) reduce to vapor-vapor and vapor-solid assembly limits. The complete velocity and pressure fields may be computed easily from Eqs. (9) to (12).

IV. RESULTS AND DISCUSSION

Simple exact solutions for the flow fields in and around a compound droplet submerged in extensional and paraboloidal flows have been found in the previous sections. We are now in a position to examine the other important physical quantities such as drag force and stresslet coefficient for the two-sphere assembly. Since we have determined the solutions in singularity form, it is a straightforward task to derive formulas for these physical quantities directly without integrating the surface stresses. The strengths of the total Stokeslets determine the drag force and for the extensional flow we find the drag force D_e from Eq. (21) to be

$$\frac{D_e}{8\pi\mu^{(1)}\alpha b^2} = \frac{\beta'}{\beta} \left[\frac{3\Lambda}{2} \left(1 - \frac{1}{\beta'^5} \right) + (1 - \Lambda) \left(1 - \frac{1}{\beta'^3} \right) \right]. \tag{25}$$

We see that the drag force depends on many parameters such as $\beta = b/a$, the distance $c = a\sqrt{1 + \beta^2} = a\beta'$ between the centers, rate of shear α , and the viscosity parameter Λ . This drag perhaps arises due to the geometrical asymmetry. This geometrical asymmetry vanishes in the limiting cases: (i) $a = 0, b > 0$; and (ii) $b = 0, a > 0$. In these limiting cases, we expect the drag to be zero provided the origin about which θ is measured (see Fig. 1) is at the center of the sphere. In fact, we see from Eq. (25) that this drag force is indeed zero for $b = 0$ as expected. However, it is nonzero for $a = 0$ because the origin shifts in this case and is no more at the center of the sphere. Figure 4 shows the plots of nor-

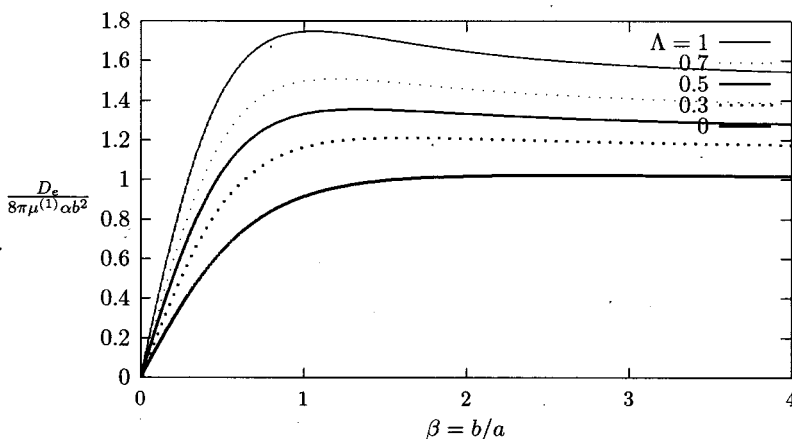


FIG. 4. Drag force in extensional flow.

malized drag force $D_e/8\pi\mu^{(1)}\alpha b^2$ versus $\beta=b/a$ for several values of the viscosity parameter $\Lambda:0.0, 0.3, 0.5, 0.7,$ and 1.0 . It shows that the normalized drag force increases with Λ for any fixed value of the parameter β . It is worth noting that the normalized drag force is maximum at $\beta\approx 1$ for all values of $\Lambda\leq 1.0$.

It is of some interest to calculate the stresslet coefficient for a force-free compound droplet. The solution for a force-free droplet may be obtained by subtracting the translational velocity (arising in Stokes problem) from Eqs. (21) to (22). For a force-free droplet, the sum of the translational and extensional contributions to the drag must vanish, namely $D_e+D_t=0$. The expression for D_t is [Eq. (28) in Ref. 16]

$$\frac{D_t}{2\pi\mu^{(1)}U_a} = 2 + \Lambda \left(3\beta - \frac{\beta}{\beta'} \left(3 - \frac{\beta^2}{\beta'^2} \right) \right) + (1 - \Lambda) \left(2\beta - \frac{2\beta}{\beta'} \right). \tag{26}$$

The required translational velocity U can now be found from Eqs. (25) and (26). Solutions (21)–(22) are now modified in accordance with this zero drag condition and the stresslet dominates the flow field in the case of a force-free droplet. The effective stresslet coefficient is

$$\frac{S_e}{\alpha a^3} = 2\beta\beta' \frac{\frac{3\Lambda}{2} \left(1 - \frac{1}{\beta'^5} \right) + (1 - \Lambda) \left(1 - \frac{1}{\beta'^3} \right)}{\left[2 + \Lambda \left(3\beta - \frac{\beta}{\beta'} \left(3 - \frac{\beta^2}{\beta'^2} \right) \right) + (1 - \Lambda) \left(2\beta - \frac{2\beta}{\beta'} \right) - \frac{\beta}{\beta'^2} \right]} \left[\Lambda \left(\frac{\beta^3}{\beta'^3} + \frac{3}{2}\beta\beta' - \frac{\beta}{\beta'^2} \left(3 - \frac{\beta^2}{\beta'^2} \right) \right) + (1 - \Lambda) \left(\beta\beta' - \frac{\beta}{\beta'^2} \right) - \left[1 - \Lambda \left(-\frac{3}{2}\beta\beta'^2 + \frac{3\beta}{2\beta'^5} - \frac{5}{2}\beta^3 + \frac{\beta^3}{2\beta'^3} \left(\frac{9}{\beta'^2} - 2 \right) \right) + (1 - \Lambda) \left(\beta^3 + \frac{\beta^3}{\beta'^3} + \beta\beta'^2 - \frac{\beta}{\beta'^3} \right) \right] \right]. \tag{27}$$

Note that the first term on the right hand side of Eq. (27) is due to the subtraction of the translational velocity. The stresslet coefficient plays a very important role in the theory of viscosity of suspensions in rheology. However, we will not proceed here to calculate the effective viscosity but discuss in brief the stresslet coefficient for two extreme values of the viscosity parameter $\Lambda:0$ and 1 .

A. Vapor–solid assembly $\Lambda = 1$

The effective stresslet coefficient S_e^R in this case is

$$\frac{S_e^R}{\alpha a^3} = 3\beta\beta' \frac{\left(1 - \frac{1}{\beta'^5} \right)}{\left[2 + 3\beta - \frac{\beta}{\beta'} \left(3 - \frac{\beta^2}{\beta'^2} \right) \right]} \left[\left(\frac{\beta^3}{\beta'^3} + \frac{3}{2}\beta\beta' - \frac{\beta}{\beta'^2} \left(3 - \frac{\beta^2}{\beta'^2} \right) \right) - \left[1 + \frac{3}{2}\beta\beta'^2 - \frac{3\beta}{2\beta'^5} + \frac{5}{2}\beta^3 - \frac{\beta^3}{2\beta'^3} \left(\frac{9}{\beta'^2} - 2 \right) \right] \right]. \tag{28}$$

We note that $S_e^R = -\alpha a^3$ when $b=0$ as it should be for a single bubble. For $a=0$, $S_e^R = -\frac{5}{2}b^3$ and we recover the Einstein viscosity coefficient for a rigid sphere.

B. Vapor–vapor assembly $\Lambda = 0$

This corresponds to the case of composite bubbles. A brief discussion on composite bubbles and the forces molding them is provided in Boys.²³ From Eq. (27) we see that the stresslet coefficient now becomes

$$\frac{S_e^V}{\alpha a^3} = - \left[1 + \beta^3 + \frac{\beta^3}{\beta'^3} + \frac{\beta}{\beta'^2} \frac{\beta'^5 - 1 - \beta^5}{\beta' + \beta\beta' - \beta} \right]. \tag{29}$$

Since many similarities between Stokes flow and electrostatics is well known in the literature, it may be worthwhile to point out few such similarities noticed here. Firstly, the above result differs only in sign from the polarizability of the conducting double sphere in electrostatics.²⁴ Second, the dipole moment in electrostatics is independent of the choice of coordinate system and so is the stresslet coefficient for a vapor–vapor assembly. It should be pointed out that the vapor–vapor assembly corresponds to zero-viscosity limit (i.e., $\mu^{(2)}\rightarrow 0$) compound droplet. However, the physical realization of such a vapor–vapor assembly with sharp edges has not been achieved (except for soap bubbles²³) yet to the best of our knowledge. Hence, these results for vapor–vapor assembly appear to be of limited significance at the present time.

Now we discuss briefly the drag in paraboloidal flows. In the case of a compound droplet submerged in paraboloidal flow, the drag is

$$\frac{D_p}{16\pi\mu^{(1)}Kb^3} = \Lambda \left(1 - \frac{1}{\beta'^5} \right). \tag{30}$$

It follows from this equation that the drag force is zero for a vapor–vapor assembly and it is maximum for vapor–solid assembly. In fact, it shows that the drag force increases monotonically with Λ for a fixed vapor–liquid droplet. We have plotted the normalized drag force $D_p/16\pi\mu^{(1)}Kb^3$ against $\beta=b/a$ for several values of the viscosity parameter $\Lambda:0.1, 0.3, 0.5, 0.7,$ and 0.9 in Fig. 5. It shows that the normalized drag very quickly (with b/a) approaches its

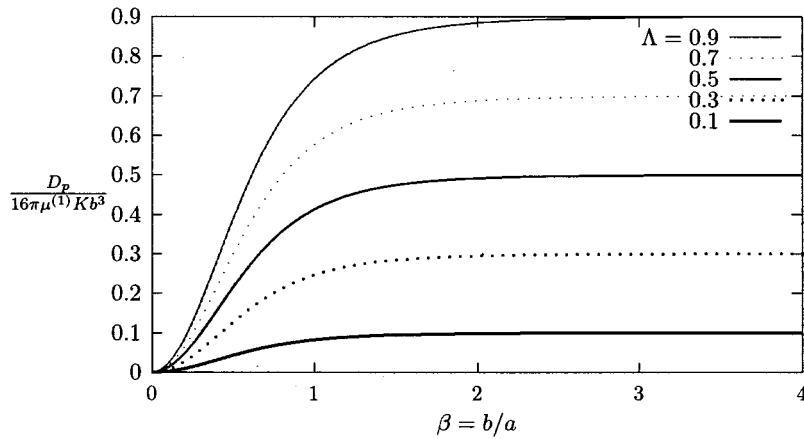


FIG. 5. Drag force in paraboloidal flow.

maximum value. The maximum value depends on the viscosity ratio and significantly on the liquid volume in the dispersed phase. We notice from this figure that for larger values of Λ , the maximum value of this drag force is attained when the volume of the liquid sphere is much greater than the vapor volume in the two-sphere assembly.

V. FURTHER FEATURES OF DRAG FORCE IN EXTENSIONAL FLOWS

The drag in extensional flow significantly depends on the choice of the origin. We shall now illustrate this by choosing the origin at D , i.e., at the center of the contact circle. The governing differential equations are the same as they are invariant under translation of origin and the complete solutions can be derived by the use of sphere theorems as explained in Sec. III A. It can be seen that the shift of origin strongly influences the strength of primary image singularities such as Stokeslet, stresslet and potential-doublet and further introduces an extra Stokeslet at O . The higher order singularities, however, remain unaffected. For the sake of brevity we omit the details and focus our attention on the expression for the drag which is found to be

$$\frac{D_{eD}}{8\pi\mu^{(1)}\alpha b^2} = \frac{\beta}{\beta'} \left[1 - \frac{1}{\beta^3} + \frac{\Lambda}{2\beta'^3}(\beta'^3 + 2) \right], \quad (31)$$

where the second suffix D indicates that the origin is taken at this point. Clearly, Eqs. (25) and (31) are quite different and interestingly the latter reveals the existence of zero drag corresponding to equilibrium. We observe that the shifting of origin alone does not make the drag zero. Rather, the equilibrium position (for which the force vanishes) depends on the viscosity and radii ratios. The plots shown in Fig. 6 further illustrates these features. The various values for which the force vanishes may be obtained by equating Eq. (31) to zero which yields the following relation between viscosity parameter Λ and ratio of radii parameter $\beta = b/a$:

$$\Lambda = \frac{2\beta'^3(1 - \beta^3)}{\beta^3(\beta'^3 + 2)}. \quad (32)$$

The above expression yields the critical value β_c of β for which the drag vanishes at a specified value of Λ . Since Λ lies between 0 and 1, Eq. (32) gives the constraint $\beta_c \leq 1$ or equivalently $b \leq a$. This in turn implies that the liquid volume should be less than the vapor volume in order to have a vanishing drag force. It also follows from Eq. (32) that β_c is an increasing function of Λ (see Fig. 6) with $\beta_c = 0.7965595828$ for $\Lambda = 1$ and $\beta_c = 1$ for $\Lambda = 0$. In other words, when the sphere S_b is also a vapor ($\Lambda = 0$), the drag becomes zero if the two radii of the spheres are equal which corresponds to the case of composite bubbles. Due to the

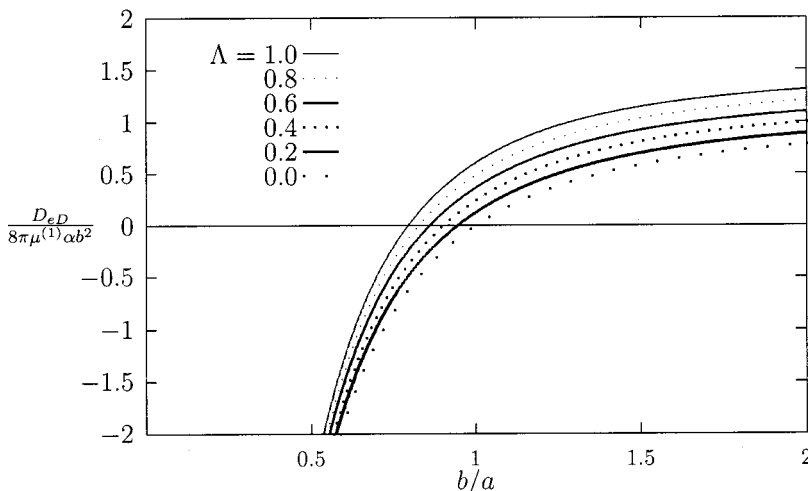


FIG. 6. Drag force in extensional flow with origin at the center of the circle of intersection of two spheres.

added symmetry about the plane of intersection in this case, one would expect this result to be true even for the case of arbitrary contact angle. For the vapor–solid assembly ($\Lambda = 1$), the force vanishes when $b/a = 0.796\,559\,582\,8$. In all cases for which the drag force is zero, the stresslet coefficient follows directly from the solution without subtracting the translational velocity.

It is also of interest to analyze the stability of the equilibrium (zero drag) position found above. The stability issue concerning compound drops has been addressed by many workers in variety of circumstances. The review on compound multiphase drops by Johnson and Sadhal⁴ provides references to various earlier works on the stability of such drops. A later work by Sadhal and Oguz²⁵ analyzed the stability of a completely engulfed drop/bubble suspended in uniform flow of a viscous fluid. The cited authors examined the translatory motion of a compound drop—consisting of a liquid drop/bubble completely engulfed by a larger spherical surface containing another immiscible liquid—in a distinct third liquid. By balancing the viscous drag with a suitable buoyant force, they found stable, unstable and metastable equilibrium positions of the inner sphere with respect to the outer spherical surface. Following their work, we provide here a brief discussion on the stability of the zero drag position of the compound drop Γ (Fig. 1) in extensional flow.

We first observe that in extensional flow the equilibrium results even in the absence of buoyant force and Eq. (32) gives the values of Λ and β corresponding to equilibrium for which the drag force vanishes. The stability of this zero drag position can be analyzed by moving the origin along z -direction. We noticed in the beginning of this section that the shifting of origin along z -axis changes the drag force significantly. It can be seen from Eqs. (25) and (31) that for a given equilibrium value of Λ and β with $\alpha > 0$, moving the origin towards O results a drag force along positive z -direction. Similarly it can be shown that moving the origin towards O' leads to a drag force along negative z -direction. Therefore, the equilibrium in this case is clearly stable. For the same equilibrium values of Λ and β with $\alpha < 0$, a similar examination shows unstable equilibrium.

Equations (31) and (32) point out yet another feature in Stokes flow. It is obvious that the drag force is positive for $\beta > \beta_c$ (at which the force is zero) and is negative for $\beta < \beta_c$. This is due to the change of sign of the total image Stokeslets leading to the so called “Stokeslets reversal” phenomenon. Indeed, the reversal phenomenon has been noticed in Stokes flow²⁶ recently in the context of point force images in a spherical container. The reversal of image Stokeslets will change the direction of the force and arises mainly due to the geometrical effect in the present case. This phenomenon can be eliminated in two ways viz. (i) by choosing the liquid volume larger than the vapor volume, and (ii) by placing the origin of the configuration at one of the centers of the spheres. These rules may perhaps have a general validity for arbitrary contact angle.

VI. CONCLUSION

Simple analytical solutions are obtained for the problem of Stokes flow in and around a compound (hybrid) droplet

suspended in nonuniform flow fields. By repeated application of sphere theorems, the solutions are found in singularity form for the droplet placed in axisymmetric extensional and paraboloidal flows. It is found that the dimensionless viscosity ratio Λ and the dimensionless parameter $\beta = b/a$ (ratio of radii) strongly influence the flow field, the drag, and the stresslet coefficient. The drag force in extensional flow is shown to be significantly dependent on the choice of the origin. If the origin is chosen at the center of the circle of intersection, then the drag vanishes at a critical value $\beta = \beta_c$ which depends on Λ . The reversal phenomenon is exhibited when β goes through those critical values. Two rules are proposed for eliminating this reversal effect which may perhaps have a general validity. The solutions for more complicated axisymmetric flows in the presence of a compound droplet can be obtained in a similar fashion. Finally, the configuration considered here is special because the two spheres share a common inverse point that admits elegant solutions. However, as evidenced from the present results, the typical features of the flow can be observed even with the limited constraint $c^2 = a^2 + b^2$. Furthermore, the comparison of streamlines for pure translation presented in Palaniappan and Kim¹⁶ and Vuong and Sadhal¹⁷ shows that the contact angle does not influence significantly the flow fields in and around the compound droplet. Therefore, the orthogonality constraint may not be excessively restrictive. The relaxation of the this constraint will introduce contact angle as an additional parameter and in this case the problem may be solved by the use of conical functions in toroidal coordinates. In such investigations, the solutions and the physical quantities will contain infinite integrals involving complicated functions which have to be evaluated numerically.

ACKNOWLEDGMENTS

The first author (D.P.) thanks the Alexander von Humboldt foundation for financial support and the second author (P.D.) thanks Texas Advanced Research Program for financial support under Grant No. TARP-97010366-030. The authors are grateful to the reviewers for helpful suggestions.

¹E. Evans and D. Needham, “Attraction between lipid bilayer membranes in concentrated solutions of nonadsorbing polymers: Comparison of mean-field theory with measurements of adhesion energy,” *Macromolecules* **21**, 1822 (1988).

²E. Evans, D. J. Klingenberg, W. Rawicz, and F. Szoka, “Interactions between polymer-grafted membranes in concentrated solutions of free polymer,” preprint (1996).

³C. T. Avedisian and R. P. Andres, “Bubble nucleation in superheated liquid-liquid emulsions,” *J. Colloid Interface Sci.* **64**, 438 (1978).

⁴R. E. Johnson and S. S. Sadhal, “Fluid mechanics of compound multiphase drops and bubbles,” *Annu. Rev. Fluid Mech.* **17**, 289 (1985).

⁵S. S. Sadhal, P. S. Ayyaswamy, and J. N. Chung, *Transport Phenomena with Drops and Bubbles* (Springer-Verlag, New York, 1997).

⁶T. B. Jones, “Effective dipole moment of conducting intersecting spheres,” *J. Appl. Phys.* **62**, 362 (1987).

⁷A. V. Radchik, A. V. Paley, G. B. Smith, and A. V. Vagov, “Polarization and resonant absorption in intersecting cylinders and spheres,” *J. Appl. Phys.* **76**, 4827 (1994).

⁸G. G. Stokes, “On the effect of the internal friction of fluids on pendulums,” *Trans. Cambridge Philos. Soc.* **9**, 8 (1851).

⁹H. Lamb, *Hydrodynamics* (Dover, New York, 1932).

¹⁰J. Happel and H. Brenner, *Low Reynolds Number Hydrodynamics* (The Hague, Martinus Nijhoff, 1983).

- ¹¹S. Kim and S. J. Karrila, *Microhydrodynamics: Principles and Selected Applications* (Butterworth-Heinemann, Boston, 1991).
- ¹²C. Pozrikidis, *Boundary Integral and Singularity Methods for Linearized Viscous Flow* (Cambridge University Press, Cambridge, 1992).
- ¹³H. A. Lorentz, "A general theorem concerning the motion of a viscous fluid and a few consequences derived from it," *Zittingsverlag. Akad. Wet. Amsterdam* **5**, 168 (1897).
- ¹⁴A. T. Chwang and T. Y. Wu, "Hydromechanics of low-Reynolds number flow. Pt. 2: Singularity method for Stokes flow," *J. Fluid Mech.* **67**, 787 (1975).
- ¹⁵L. E. Payne and W. H. Pell, "The Stokes flow problem for a class of axisymmetric bodies," *J. Fluid Mech.* **7**, 529 (1960).
- ¹⁶D. Palaniappan and S. Kim, "Analytic solutions for Stokes flow past a partially encapsulated droplet," *Phys. Fluids A* **9**, 1218 (1997).
- ¹⁷S. T. Vuong and S. S. Sadhal, "Growth and translation of a liquid-vapor compound drop in second liquid. Part 1. Fluid mechanics," *J. Fluid Mech.* **209**, 617 (1987).
- ¹⁸P. C. H. Chan and L. G. Leal, "A note on the motion of a spherical particle in a general quadratic flow of a second order fluid," *J. Fluid Mech.* **82**, 549 (1977).
- ¹⁹L. G. Leal, "Particle motions in a viscous fluid," *Annu. Rev. Fluid Mech.* **12**, 435 (1980).
- ²⁰D. Leighton and A. Acrivos, "Measurement shear-induced self-diffusion in concentrated suspension of spheres," *J. Fluid Mech.* **177**, 109 (1987).
- ²¹X. Li and C. Pozrikidis, "Shear flow over a liquid drop adhering to a solid surface," *J. Fluid Mech.* **265**, 1 (1995).
- ²²D. Palaniappan, S. D. Nigam, and T. Amaranath, "A theorem for a fluid sphere in Stokes flow," *J. Aust. Math. Soc. B, Appl. Math.* **35**, 335 (1994).
- ²³C. V. Boys, *Soap Bubbles and the Forces which Mould Them* (Dover, New York, 1959).
- ²⁴D. Palaniappan and B. U. Felderhof, "Electrostatics of the conducting double-sphere," *J. Appl. Phys.* **86**, 3418 (1999).
- ²⁵S. S. Sadhal and H. N. Oguz, "Stokes flow past compound multiphase drops: The case of completely engulfed drops/bubbles," *J. Fluid Mech.* **160**, 511 (1985).
- ²⁶C. Maul and S. Kim, "Image of a point force in spherical container and its connection to the Lorentz reflection formula," *J. Eng. Math.* **30**, 119 (1996).